Wood Sci Technol (2012) 46:243–256
DOI 10.1007/s00226-011-0410-6

ORIGINAL

Adhesive penetration in beech wood: experiments

Philipp Hass · Falk K. Wittel · Miller Mendoza · Hans J. Herrmann · Peter Niemz

Received: 17 March 2010 / Published online: 6 March 2011

Abstract A study with synchrotron radiation X-ray tomographic microscopy (SRXTM) of PUR, PVAc, and UF adhesive bond lines in beech wood, bonded under various growth ring angles, is presented. The bond line morphologies and the adhesive penetration into the wood structure were evaluated after determining the hardening characteristics of the adhesives. Distinct bond line imperfections were found for the different adhesive systems. To describe the adhesive distribution inside the bond line, the saturation of the pore space instead of the commonly used maximum penetration depth seems to be adequate.

Introduction

Modern timber engineering greatly relies on wood adhesive bonding. The majority of highly engineered wood-based products have been developed on the principle of cutting wood into smaller pieces and joining them again by adhesive bonding. In this way, the natural anisotropy of wood can be reduced, and larger dimensions of structural elements with improved characteristics become possible. Even though bonding of wood elements is a rather simple processing step, the details of the penetration of the hardening adhesives into the porous wood skeleton on the several hierarchical levels (from microscopic to macroscopic) are rather complicated. It is strongly influenced by: (i) wood factors such as wood species, anatomical orientation, or surface roughness, (ii) adhesive factors such as type of adhesive or viscosity, and (iii) process factors such as applied pressure or temperature, which have a significant influence on the bonding performance (Kamke and Lee 2007).

Former studies on adhesive penetration were mainly performed using microscopy of cross-sections and micro-slides (Kamke and Lee 2007; Sernek et al. 1999;

P. Hass (✉) · F. K. Wittel · M. Mendoza · H. J. Herrmann · P. Niemz
Institute for Building Materials, ETH Zurich, Schafmattstrasse 6, 8093 Zurich, Switzerland
e-mail: phass@ethz.ch

Suchsland 1958). More integral studies were performed using porosimetry (Wang and Yan 2005) or neutron radiography (Niemz et al. 2004). To measure adhesive penetration of cell walls, scanning thermal microscopy (SThM) was used (Konnerth et al. 2008). In most cases, the penetration behavior of an adhesive is described using the maximum penetration depth, without differentiating between wood species. The differences of the penetration behavior between different wood species are demonstrated in Fig. 1, where bond lines of a PUR prepolymer are shown for softwood (Fig. 1 left) and hardwood (Fig. 1 right), both recorded in a scanning electron microscope (SEM).

In softwood, tracheids filled with adhesive are visible as a more or less interconnected zone. Hence, for softwood it seems probable to express the penetration behavior by the maximum penetration depth via a simple trigonometric relation describing the filling of uni-directional tracheids that are cut at the bond line (Suchsland 1958). For hardwood, the picture is far more complicated, as many vessels filled with adhesive appear to be isolated from the bond line. The maximum penetration depth seems to be an arbitrary measure and not suitable to describe the penetration behavior. Hence, a different approach for better characterization of the adhesive penetration has to be found, considering the anatomical structure of the specimen.

In this work, a systematic study of adhesive penetration into beech (*Fagus sylvatica* L.) samples is described. Specimens are bonded with parallel longitudinal axes under varying growth ring angles using three different adhesive systems with different initial viscosities. In order to measure the internal distribution of the adhesives in the interphase formed by the penetration of the adhesive, tomographic imaging via synchrotron radiation is used. Due to the high resolution, 3D data qualitative investigations of the bond line are feasible, which allow, for example, the detection of flaws resulting from the curing process. Performing image processing (image transformation, spatial convolution on 3D data, segmentation, and morphologic operations) leads to the segmentation of the adhesive and the pore space.

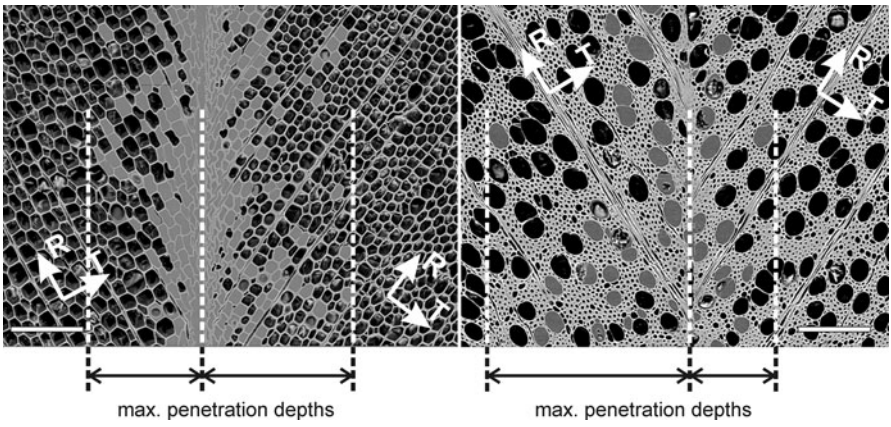

Fig. 1 SEM images of PUR prepolymer *bond lines* in spruce (*left*) and beech wood (*right*). The length of the *white bar* corresponds to 200 µm

Thereby, it is possible to characterize the adhesive penetration as the saturation of the accessible pore space.

Materials and methods

In order to provide a sound basis for an adhesive penetration model, it is necessary to characterize the given wood anatomy including (i) the pore space (see Hass et al. 2010) and the ray distribution, (ii) the viscosity evolution of the adhesive, and (iii) the bond line morphology. The following definitions for the regions inside the adhesive bond area were used:

- The bond line is the whole region, where adhesive is present. This includes the pure adhesive between the two adherents as well as the area, where the adhesive has penetrated into the wood structure.
- The adherents are the wood elements, which have been connected by the adhesive.
- In the case of polyurethane adhesives, only prepolymers were used in this study. Therefore, here the abbreviation PUR corresponds to polyurethane prepolymers.

Adhesive systems

To gain a general idea about the penetration process of adhesives into wood and the differences between various adhesives, three major adhesive types were investigated. An overview of the adhesive characteristics and their chemical composition is given for example in Dunky and Niemz (2002) or Habenicht (2006).

- Urea formaldehyde (UF) is considered to be the most important amino resin bonding agent in the area of manufactured wood products for internal use without high moisture exposure. Hardening of UF is due to a hardener activated reaction, where UF resins continue to react by polycondensation to the hardened state and are accompanied by a partially loss of water. The hardened adhesive builds insolvable and infusible spatial networks, leading to brittle, duroplastic behavior of the bond line.
- Polyvinyl acetate (PVAc) is the second most important adhesive group for the furniture industry. Solidification of PVAc is characterized by a physical process, initiated by the loss of the water contained in the adhesive dispersion. Under the consolidation pressure applied on the adherents, an adhesive film is formed and repulsive forces between the single PVAc molecules are resolved and the adhesive layer becomes solid.
- One-component polyurethane has gained in importance for load-bearing timber structures and solid wood constructions. One of the main differences between polyurethane adhesives and traditional bonding agents lies in the solid content. While the solid contents of PVAc and UF adhesives are only 50–70%, polyurethanes contain no solvents and therefore exhibit a solid content of 100%. They consist basically of polyol-isocyanate prepolymers with active isocyanate

groups, which react with the moisture of the wood creating CO_2 and also partly with the OH groups of the adherent surfaces. Adhesive viscosity can be adjusted by the addition of organic solvents and the proper molar mass of the prepolymer. However, polyurethane prepolymers as used in this study contain no additives such as fillers or defoamers that are added in ready-for-sale adhesives.

Hardening

In a further step, the hardening behavior of the pure adhesives was investigated. UF mixtures of 100 g UF adhesive powder plus 80, 70, 60, and 50 ml of water were prepared. The UF powder, already containing the hardener, is suitable as a cold-hardening system. Evolution of viscosity and temperature of the different mixtures were tracked using a rotational viscosimeter (Haake Viscotester VT5R) and a thermometer (Fig. 2).

The measured temperature changes during hardening stayed below 1°C and are negligible. For PUR and PVAc, such measurements are not possible; PUR becomes foamy during hardening, while PVAc builds a skin on the surface of the sample that prevents further loss of water from the mixture to the atmosphere. Hence, the viscosity of the adhesive under the skin stays almost constant. However, the measurements for PVAc can be performed inversely. Since the solidification of PVAc depends on the loss of the water, the change in solid content and thereby in viscosity can be used to describe the solidification process, but only if the parameters for the water uptake by the wood are known as well. In order to monitor this dependence of the viscosity on the solid content, water was added stepwise to the PVAc type with the higher initial viscosity (due to its higher solid content), until the solid content of the second mixture was reached (Fig. 3).

Bond line morphology

For the investigation of the volumetric distribution of the adhesives inside the wood after hardening, μ-tomography was conducted on bonded beech samples using

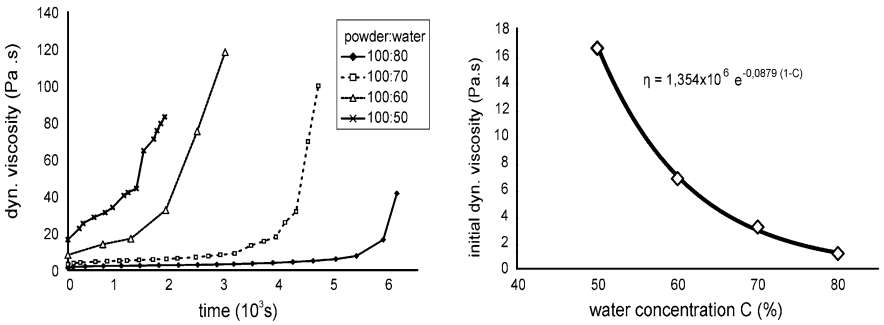

Fig. 2 (*left*) Evolution of the dynamic viscosity of hardening UF adhesives with different solvent content and (*right*) initial viscosity

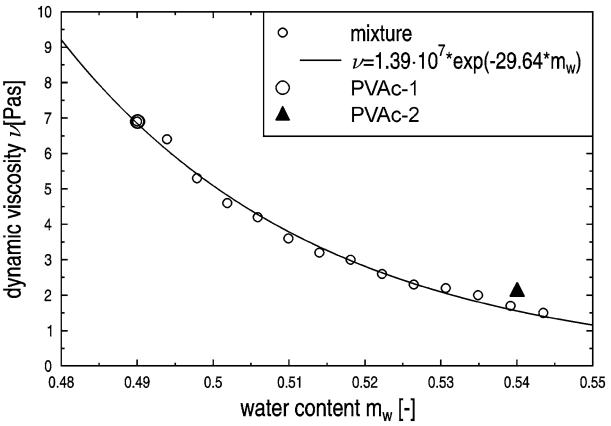

Fig. 3 Evolution of the dynamic viscosity of PVAC with differing water:solid ratio

synchrotron radiation X-ray tomographic microscopy (SRXTM). The influence of the anatomical direction on the adhesive penetration was determined by using various growth ring angles (GRA) from radial to tangential orientation in 15° steps during bonding (Fig. 4), while keeping the longitudinal axes parallel. To allow a later comparison to the failure behavior and the strength of the bonds, the samples for the tomographic measurements were chosen from lap-shear specimens used in Hass et al. (2009). From the three PUR variations used in that paper, only specimens bonded with PUR-1 and PUR-2 were used. In both types of PUR, the isocyanate content (NCO) and the amount of urethane groups (U) were the same (NCO: 16%; U: 0.58 mol/kg). They differed in their initial viscosity (PUR-1: 1310 mPas; PUR-2: 5460 mPas), their reactivity (film formation time: PUR-1: 300 min; PUR-2: 420 min), and their cross-linking density after hardening (PUR-1: 0.22 mol/kg; PUR-2: 1.25 mol/kg). For PVAc and UF, both adhesive variants per system used in Hass et al. (2009) were investigated. These variants differed only in their solid content and therefore in their initial viscosity (PVAc 1: 2380 mPas; PVAc 2: 6900 mPAs; UF-1: 1860 mPas; UF-2: 4220 mPas). To ensure the same amount of adhesive in the cured bond line, the amount of applied adhesive was adjusted. A detailed description of the procedure can be found in Hass et al. (2009). This gave a total number of 42 specimens, which were surveyed using synchrotron radiation X-ray tomographic microscopy (SRXTM). The details of the investigation method are described in Hass et al. (2010), which is based on the same set of samples as used for this study. Today, SRXTM is still a relatively novel technology that does not yet allow huge sample size studies. Facilities to perform such measurements are scarce, and an enormous amount of data has to be processed for measurement, reconstruction, and evaluation. By choosing only one sample per adhesive and GRA step, a well-founded statistical investigation on the influence of the GRA unfortunately is not possible; since the aim of this survey was the investigation of the major principles of the penetration behavior, an increased number of influencing factors were preferred rather than a higher number of repetitions.

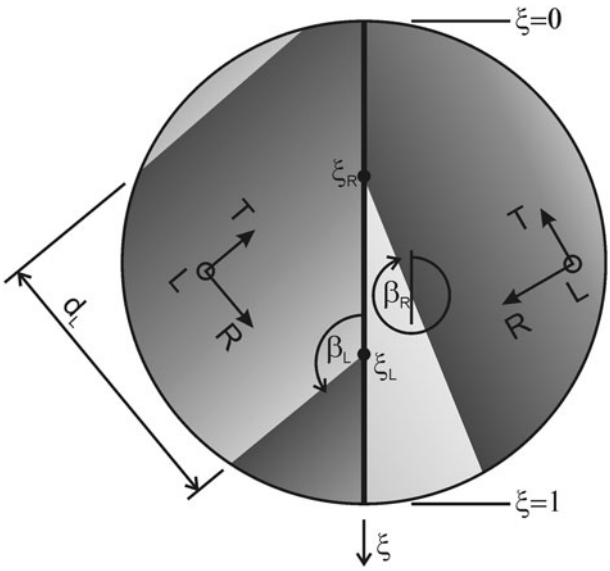

Fig. 4 Definition of growth ring orientations and positions in local coordinates of a cylindrical specimen. Signs and symbols: *R*/*T*/*L* radial/tangential/longitudinal direction, β growth ring angle, d growth ring width, ξ position in *bond line*, subscriptions: *L* left side, *R* right side

The μ-CT data consist of a stack of images of cross-sections in the RT plane averaging a volume of 3.7 μm^3 by one scalar gray value. Several image processing steps were applied to analyze the image stacks, which are explained in the following and that were all conducted using the image processing tools from the software package MatLab. First, all images are rotated in the uniform coordinate system (Fig. 4) using a bicubic interpolation method. Since rotating the image does not allow a direct assignment of gray scale values for each rotated pixel, this procedure uses a weighted average of pixels in the nearest neighborhood to determine the gray scale value of the rotated pixel (MatLab Documentation 2009; Gonzales et al. 2009). Then, the same technique is used to double the resolution of the image. In a next step, the values of the gray scale image are remapped, by using the value boundaries and linearly redistributing the existing values. With this adjustment, the full intensity range is used and the contrast is enhanced. Due to contrast shifts along the longitudinal axis, the gray value distribution is shifted. At periodic height levels (every 100th slice) gray values of pure adhesive zones are selected to obtain a sub-blockwise gray value distribution of the adhesive. These slices are used for the investigation of the adhesive penetration, by analyzing the maximum penetration depth and the adhesive saturation of the available pore space. While the pore distribution is clearly sectioned (see Hass et al. 2010), the ones for adhesives and wood strongly overlap, complicating the segmentation. The addition of a contrast enhancing substance to the adhesive, however, was dismissed due to the inherent uncertainties of this procedure. For example, Modzel et al. (2010) added rubidium to increase the X-ray attenuation of the adhesive. Unfortunately, the rubidium

penetrated deeper into the wood than the adhesive, hence questioning the suitability of this method. Apart from the possible effects for the identification of the adhesive, changes to the adhesive properties might occur.

To segment the adhesive in the data of this study, a two-step procedure was applied: first an intensity-based segmentation using a fitted normal distribution for local thresholding is performed. Here, every 50th slice of the image stack was used to determine the gray value distribution for the adhesive by manually selecting several points (at least 30), where adhesive was clearly present. Since adhesive regions are rather compact, morphologic image processing on binarized images was applied to filter small segmented zones away from the bond line inside the sub-block. Contour smoothing could be obtained by morphologic opening of connected regions (blobs), and finally small holes inside the blobs can then be filled if desired. Additionally, small blobs without depth can be deleted by a blob analysis on the segmented tomographic data (see Fig. 5).

By interpolating the picked gray scale values over the whole volume, the bond lines from the samples could be extracted. Finally, iso-surfaces of the identified adhesive were created for visualization purposes (Fig. 6).

Wood ray distribution

As proposed in Hass et al. (2010), the tangential deflection of the vessels by the wood rays is typical for beech wood. To complete the characterization of anatomical features that have an influence on the development of the bond line, the tomographic data were used to evaluate the proportion of wood rays on the total wood material. Therefore, the data sets were aligned in the LT plane, and the wood rays were identified by digital image analysis (Fig. 7). The used procedure was similar to the one used for identifying the pore space (see Hass et al. 2010) and the adhesive. However, for identification of the rays, a different feature was used. The rays appear as a checkerboard pattern, which changes from one layer to the next, and appear as

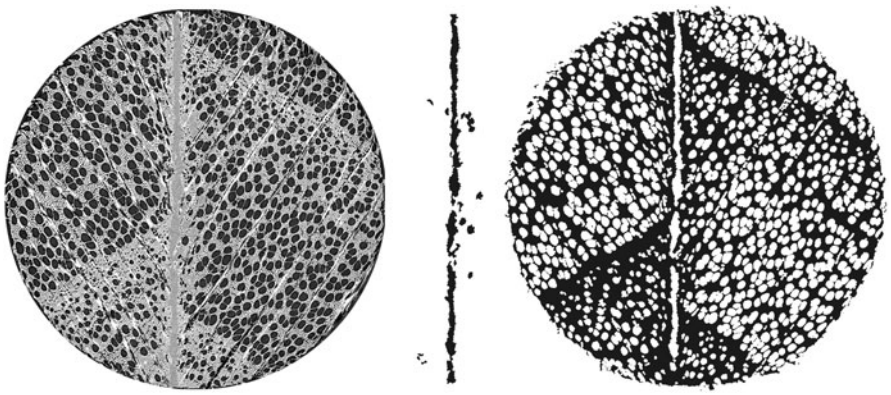

Fig. 5 *left*: μ-CT cross-section, *center*: segmented adhesive and *right*: pore space without segmented adhesive

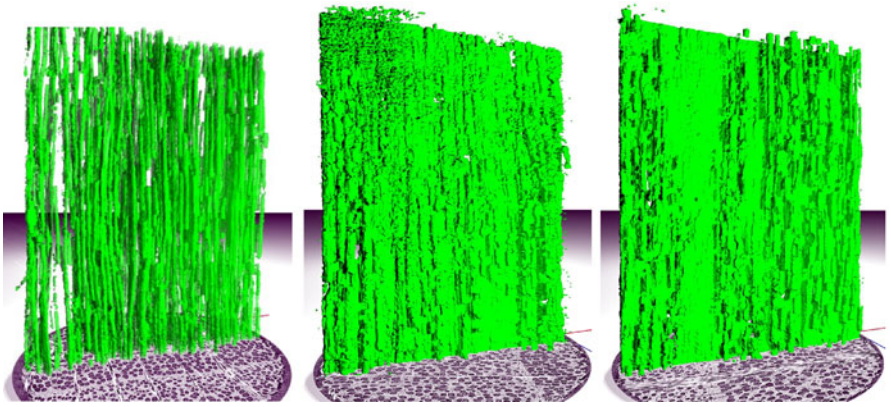

Fig. 6 Extracted *bond lines* for PUR-2 (0°), UF-1 (75°), and PVAC-2 (90°) from *left* to *right*

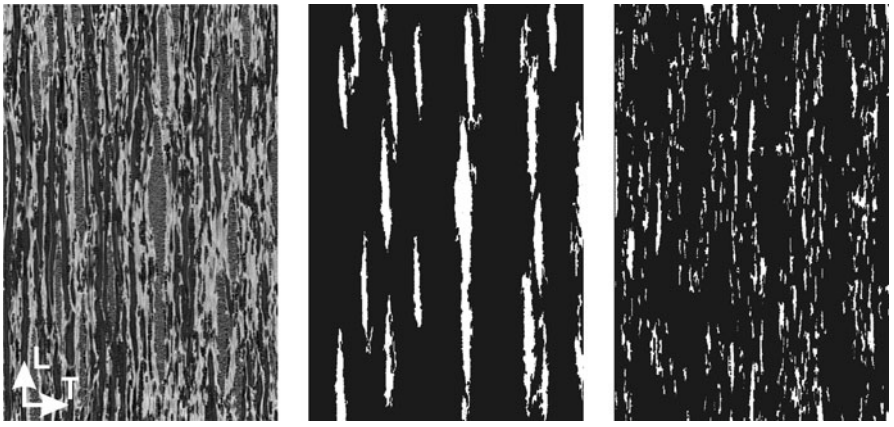

Fig. 7 Identified wood rays in beech wood in the LT plane located in early wood. *Left* layer in the RT plane, *center* the 20 largest segmented rays, *right* smaller rays. The portion of rays is 24% (compare 21% in Wagenführ 2007), and the identified grain angle was 4.3°

small blobs without depth. The ratio of these areas is determined and proved to agree very well with values given in literature (Wagenführ 2007).

Results

Adhesives penetration follows the path of lowest resistance into the porous structure, either by gross penetration or by cell wall penetration (Kamke and Lee 2007). Filling of accessible, cut cell lumen and mainly of the interconnected network of vessels was easily observed, as well as the open space between the two contacting rough surfaces. Cell wall penetration as well as penetration through pits and small cell lumen was beyond the scale of observation. The flow is initiated by

capillary suction and applied pressure. However, the local magnitude of the pressure in the volume of the sample remained unknown in these experiments due to surface roughness and the strong heterogeneity and meso structure of the wood itself. The gross penetration into beech is dominated by vessel network characteristics such as vessel diameter, density, connectivity, and alignment as well as by the temporal and spatial evolution of the viscosity of the adhesives.

When comparing the adhesive systems, even though the initial viscosity of PUR is comparable to PVAc and UF, its penetration is much deeper (Fig. 8).

This is mainly due to the fact that a pure prepolymer without fillers and additives was used. The viscosity change is only due to a polyaddition reaction and takes place long after the penetration. The fact that the penetration is rather fast can be seen when comparing the surface where the application was performed with the surface of the second adherent where no adhesive was applied. As a result, bond lines starve, which in fact is quite typical for PUR. PVAc exhibits a similar penetration behavior as UF showing a distinct bond line and only minor penetration into the pore structure, mainly filling all directly accessible volumes including cut open vessels.

The influence of the GRA on the penetration pattern is best explained at the extremes 0° and 90° (see Fig. 8). For all adhesives, it seems that the penetration is deeper at 90° than 0°, confirming observations by Sernek et al. (1999). Basically, adhesives mainly penetrate the longitudinally aligned vessels. However, as shown by Bosshard and Kucera (1973) and Hass et al. (2010), vessels in beech have a strong waviness in the tangential direction since they have to weave around the

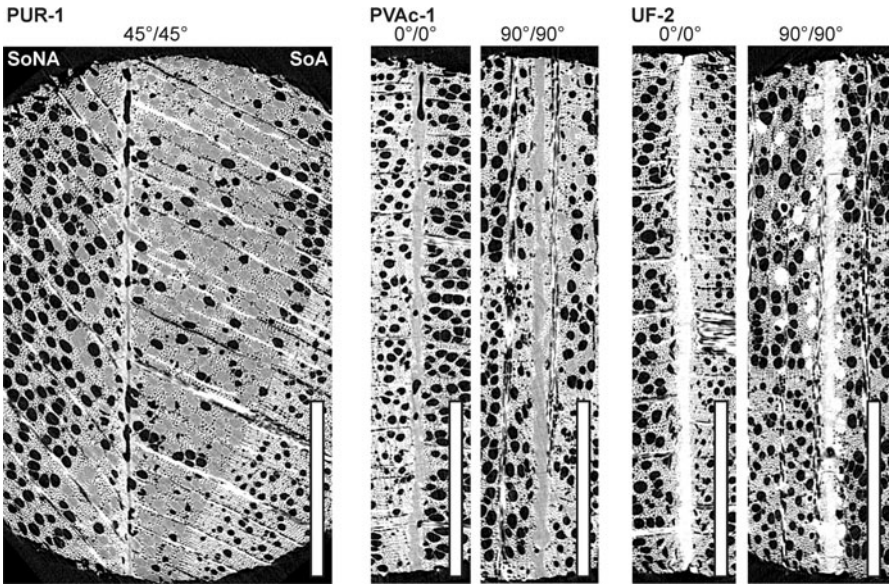

Fig. 8 Cross-sections of selected samples. The height of the *white bar* corresponds to 1 mm. Note that *gray values* of the adhesives differ, depending on their density and composition. Abbreviations: *SoNA* side of non-application, *SoA* side of application

radially directed wood rays. Therefore, when regarding cross-sections, it is obvious that the impression of a deeper penetration in the tangential direction is created. Another reason for this impression is the anatomical characteristics of beech to build a growth ring limited vessel network (Bosshard and Kucera 1973; Hass et al. 2010), which causes the growth ring border to act as a barrier for the penetration. Therefore, no vessels outside the cut growth ring are filled (Fig. 8 left). At a GRA of 90°, all growth ring borders are oriented perpendicular to the bond line, while at a GRA of 0° they are adjusted parallel to it, blocking further advancement of the adhesive from the bond line.

The established way to characterize the penetration behavior of an adhesive is the determination of the maximum penetration depth in single cross-sections. As this might be a feasible method for the penetration in softwoods, it seems inappropriate for hardwoods such as beech wood, where strongly different bond line morphologies can be observed (see comparison Fig. 1). Therefore, the saturation of the available pore space by the adhesive is proposed for characterization, which represents the ratio between the amount of adhesive and the porosity of the sample without the adhesive. The saturation can be considered to be physically more meaningful for the description of the adhesive penetration, as it takes into account the wood structure and additionally reflects the adhesive distribution between the two adherents. In Fig. 9, the two ways of determining the adhesive penetration are demonstrated on a UF bond line.

Several questionable issues about the usual investigation methods can be recognized. Firstly, the maximum penetration depth lacks important information about the bond line morphology, in regard to the penetration itself, as well as to the pure bond line between the two adherents. Hence, imperfections in the bond line, which will have a huge impact on the bond strength, are not taken into account;

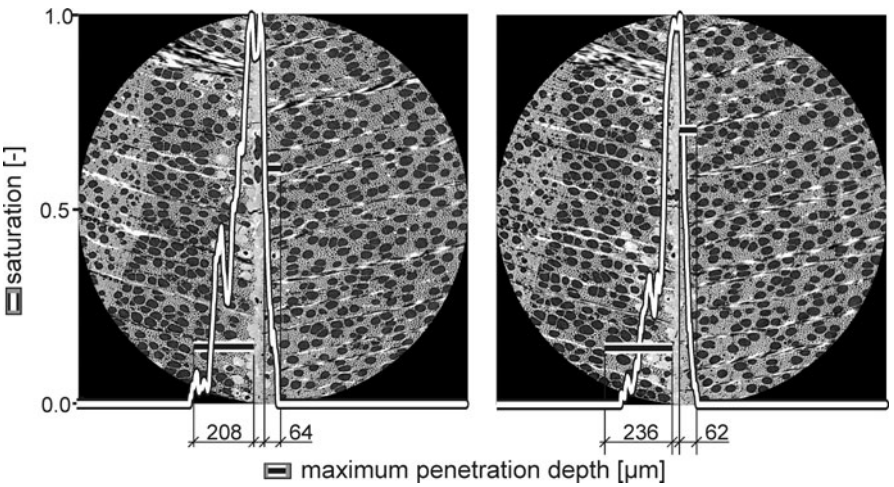

Fig. 9 Saturation and maximum penetration depth in two cross-sections of a specimen containing a *bond line* of an UF adhesive. The distance in longitudinal direction between the cross-sections is 100 slices or 370 µm

rather isolated pores filled with adhesive, whose contribution to the bond strength are questionable, define its value. Those bond line imperfections are characteristics of the adhesives: (i) for PUR, bond line starvation is typical due to the high mobility of the adhesive; (ii) for PVAc, which behaves rather ductile, formation of pores could be observed inside the bulk adhesive due to excessive shrinkage; (iii) for UF typical crack patterns due to restrained shrinkage of the brittle adhesive appear. Typical examples are shown in Fig. 10.

The example shown in Fig. 9 demonstrates how the results of the measurement depend on the investigated cross-section and how the bond line morphology changes along the longitudinal axis. Although the two cross-sections are only 370 μm apart, the maximum penetration depth on the left hand side is about 15% less and contains two large pores in the adhesive layer, resulting from the excessive shrinkage of the adhesive during hardening. Therefore, information given by single cross-sections is rather limited, while several investigations on the same bond line give a more detailed description of the bond line characteristics.

Only averages over all samples of a given adhesive can suitably demonstrate the differences between them. As the application of PUR was carried out single-sided, a differentiation between the side of application (SoA) and the side of non-application (SoNA) (see Fig. 8 left) had to be made; so all samples were arranged with the SoA on the right side. For UF and PVAc, a simplification could be made as the adhesive application was performed on both adherents, so each side of a sample could be regarded as a single measurement. This means, for the right adherent, the saturation distribution was evaluated from the right end to the middle of the pure adhesive zone; for the left adherent, the saturation was identified from the left side. Since averaging these distributions only illustrates half of the bond line, the distribution was mirrored. In Fig. 11, the mean values for the saturation and the maximum penetration depth show no distinct difference between UF and PVAc.

The saturation, however, indicates that the UF adhesives develop a bond line where the adhesive layer shows less voids, while the PVAc bond line inherits more areas with no adhesive at all, such as holes and pores. Between the two PVAc adhesives, the saturation shows differences as well. Comparing the saturation per

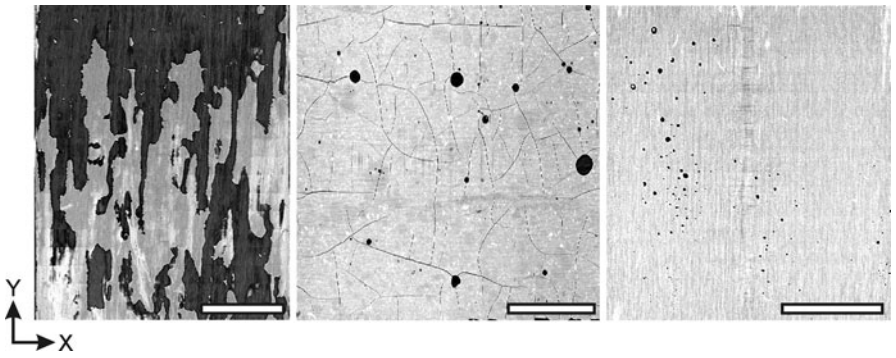

Fig. 10 *Bond line* imperfections from *left* to *right*: Starved PUR, cracked UF, and PVAC with multiple voids. The length of the *white bar* corresponds to 1 mm

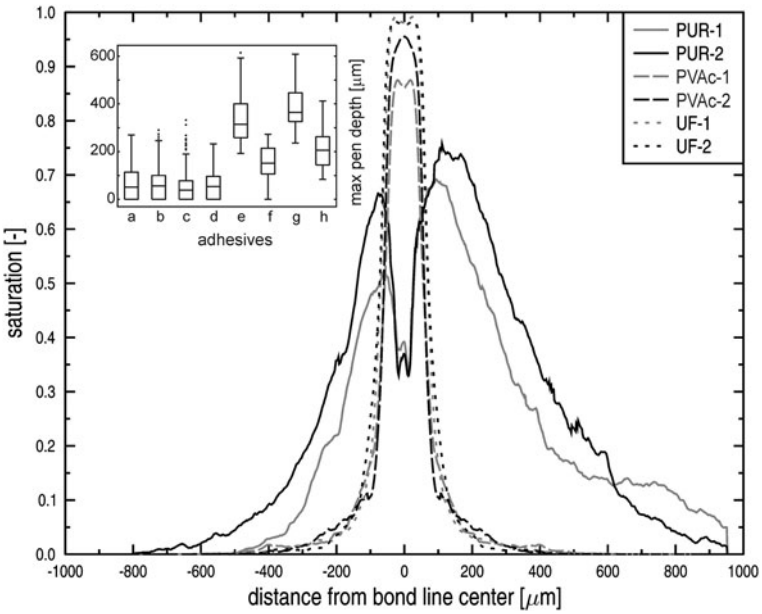

Fig. 11 Mean values for saturation and maximum penetration depth (*inset*). Abbreviations for adhesives in *inset*: *a* PVAC-1, *b* PVAC-2, *c* UF-1, *d* UF-2, *e* PUR-1 side of application (SoA), *f* PUR-1 side of non-application (SoNA), *g* PUR-2 SoA, *h* PUR-2 SoNA

adhesive with the results of the lap-shear tests in Hass et al. (2009), the same trend for the shear strength as for the saturation can be discovered. For the UF adhesives, no difference between the two viscosity steps could be detected, while for the PVAc adhesives, a significant influence of the adhesive viscosity could be found. Surprisingly, although in the PVAc-1 bond lines more voids could be detected, higher shear strength was reached with these specimens compared to those bonded with PVAc-2. It is possible that pores lead to crack arrest due to crack tip blunting, but more research on the micro-mechanical failure behavior of wood bonds is necessary to clarify these questions. The saturation explains the low wood fracture percentage of the PUR bondings in Hass et al. (2009): as the low saturation between the two adherents with these adhesives reveals that the penetration is so excessive, that the bond line partially starves, providing a weak area of preferred failure.

In a next step, the overall volume of segmented adhesive was evaluated. For UF and PVAc, the volumes are within the same range. This shows that the adjustment of the amount of applied adhesive in order to compensate for the solid content changes achieved the desired result, as the volume of the hardened adhesive in the bond line was kept nearly constant. For PUR, although the applied quantity of adhesive was equal, a difference in the volume of hardened adhesive in the bond line was observed, as more of PUR-2 was detected. As this behavior can be caused by several factors, explanations can only be speculative and more investigation is necessary to clarify the actual reason. Possible factors could for example lie in the different reaction kinetics of the two PUR or differences in the molecular chain

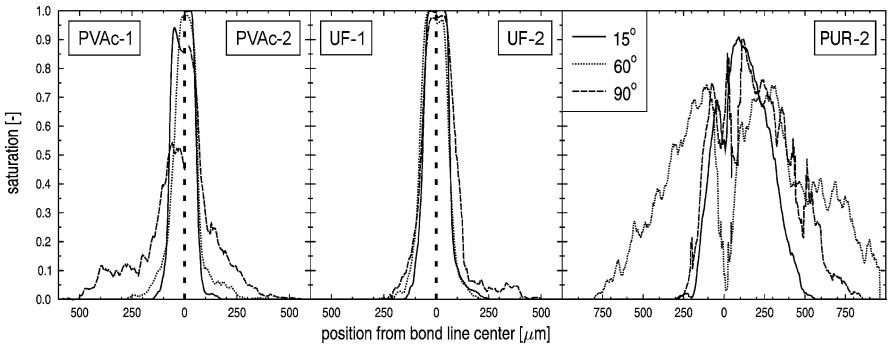

Fig. 12 Saturation profiles for three adhesive systems and different growth ring angles. Note that each *curve* is an average over 9 different regions inside one sample. PUR *curves* are rotated in a way that the application side is always on the *right*

length distribution causing the different viscosities. The different reactivities could result in differences in the structure of the cured adhesive, as the developing CO_2 is expelled at different rates. This could lead to a more foamed structure of the more reactive PUR-1, leading to a lower density. Since the viscosity is an indicator for the molecular chain length distribution, a higher fraction of shorter chains in the less viscous PUR-1 allows a penetration into smaller voids or eventually even the cell wall.

Note that the segmentation close to the contact zones of the adherents is rather difficult, since in this region cell walls typically collapse and are hard to distinguish from adhesive as their gray values are quite similar and the lumen sizes available for adhesive penetration are rather small. The resulting errors could be minimized by increasing the contrast between adhesive and wood material by, for example, using a suitable additive. But, as noted before, it is rather complicated to find such a substance without significant side effects (Modzel 2010).

The dependence on the GRA can be identified by confronting the various saturation profiles. As noted before, the sample size does not allow for a profound statistical evaluation. However, the trend was observed that PVAc and UF exhibit an increasingly wider profile for larger growth ring angles. For PUR, however, the widest saturation profiles can be found at growth ring angles between 45° and 60° (see Fig. 12).

Conclusion

The characterization of adhesive bond lines in wood by the analysis of single cross-sections in the RT plane and the determination of the maximum penetration depth lacks important information about the bond line morphology. For bond lines in softwood, this method might be sufficient, since the bond line develops a more or less interconnected and evenly distributed penetration area. In hardwoods, however, because penetration occurs mostly in the vessel network, the bond line strongly

depends on the anatomical characteristics of the wood species. Therefore, the saturation of the available pore space is proposed as a parameter, which is physically more meaningful. With this method, imperfections of the bond line are considered and the filling of single, isolated vessels is neglected, because they have only minor influence on the bonding strength. It was shown that the saturation is a suitable measure; results (bond shear strength) reported from a previous investigation (Hass et al. 2009) could be positively correlated with saturation, whereas the maximum penetration depth had no correlation with the mechanical performance.

The usage of three-dimensional data enabled the investigation of the bond line morphology at different heights of the same sample. Thereby, it became evident that bond line characteristics strongly depend on the measuring point. Therefore, the investigation of only one cross-section per sample gives limited and insufficient information about the bond line. The volumetric data also provided a look into the cured bond line presenting several imperfections that are characteristic of the different adhesive types.

Acknowledgments The financial support of this work under SNF grant 116052 is acknowledged. We are also thankful for the access to the SLS beam line TOMCAT and its crew, namely S.A. McDonald, F. Marone, and M. Stampanoni and the valuable advice on data evaluation by A. Kästner. Furthermore, we thank Purbond AG (Sempach Station, Switzerland) and Geistlich Ligamenta AG (Schlieren, Switzerland) for providing us with the adhesives.

References

Bosshard HH, Kucera L (1973) The network of vessel system in Fagus sylvatica L. Holz Roh Werkst 31:437–445

Dunky M, Niemz P (2002) Holzwerkstoffe und Leime: technologie und Einflussfaktoren. Springer, Berlin

Gonzales RC, Woods RE, Eddins SL (2009) Digital image processing using matlab, 2nd edn. Gatesmark Publishing, Knoxville

Habenicht G (2006) Kleben: grundlagen, technologien, anwendungen, 5th edn. Springer-Verlag, Berlin

Hass P, Müller C, Clauss S, Niemz P (2009) Influence of growth ring angle, adhesive system and viscosity on the shear strength of adhesive bonds. Wood Mater Sci Eng 4:140–146

Hass P, Wittel FK, McDonald SA, Marone F, Stampanoni M, Herrmann HJ, Niemz P (2010) Pore space analysis of beech wood–the vessel network. Holzforschung 64(5):639–644

Kamke FA, Lee JN (2007) Adhesive penetration of wood—a review. Wood Fiber Sci 39(2):205–220

Konnerth J, Harper D, Lee SH, Rails TG, Gindl W (2008) Adhesive penetration of wood cell walls investigated by scanning thermal microscopy (SThM). Holzforschung 62:91–98

MatLab Documentation (2009) Image processing toolbox 6.3 (2009), http://www.mathworks.com/access/helpdesk/help/pdf_doc/images/images_tb.pdf

Modzel G, Kamke FA, De Carlo F (2010) Comparative analysis of a wood: adhesive bondline. Wood Sci Technol 45(1):147–158

Niemz P, Mannes D, Lehmann E, Vontobel P, Haase S (2004) Untersuchungen zur Verteilung des Klebstoffes im Bereich der Leimfugen mittels Neutronenradiographie und Mikroskopie. Holz Roh Werkst 62:424–432

Sernek M, Resnik J, Kamke FA (1999) Penetration of liquid urea-formaldehyde adhesive into beech wood. Wood Fiber Sci 31(1):41–48

Suchsland O (1958) Über das Eindringen des Leims bei der Holzverleimung und die Bedeutung der Eindringtiefe für die Fugenfestigkeit. Holz Roh Werkst 16(39):101–108

Wagenführ R (2007) Holzatlas 6th edn. Fachbuchverlag im Carl Hanser Verlag, Leipzig

Wang WQ, Yan N (2005) Characterizing liquid resin penetration in wood using a mercury intrusion porosimeter. Wood Fiber Sci 37:505–514